

Received May 24, 2020, accepted June 1, 2020, date of publication June 18, 2020, date of current version October 1, 2020.

Digital Object Identifier 10.1109/ACCESS.2020.3003343

# Operation Mode Decision of Indoor Cleaning Robot Based on Causal Reasoning and Attribute Learning

YAPENG LI<sup>1</sup>, DONGBO ZHANG, FENG YIN, AND YING ZHANG

College of Automation and Electronic Information, Xiangtan University, Xiangtan 411105, China

National Engineering Laboratory of Robot Vision Perception and Control Technology, Xiangtan University, Xiangtan 411105, China

Corresponding author: Feng Yin (yinfeng83@126.com)

This work was supported in part by the Joint Fund for Regional Innovation and Development of NSFC under Grant U19A2083, and in part by the Science and Technology Research and Major Achievements Transformation Project of Strategic Emerging Industries in Hunan Province under Grant 2019GK4007.

**ABSTRACT** At present, the cleaning robots on market generally have the defects of simple operation mode and weak intelligence. In order to improve the intelligent degree and operation ability of cleaning robots, this paper proposes a decision method for cleaning robot's operation mode. Firstly, use the hierarchical expression ability of deep network to obtain the attributes of garbage such as state, shape, distribution, size and so on. Then the causal relationship between the attributes and the operation modes can be built by using joint learning of association attributes with depth network model and causal inference. Based on this, a fuzzy inference network for operation mode decision is designed. With the help of causal analysis, the structure of the decision model is greatly simplified. Compared with conventional fuzzy neural networks, the total parameters of the model are reduced by 2 / 3. The method proposed in this paper imitates the way that human dispose of different types of garbage and has good interpretability. The experimental results verify the effectiveness of the proposed method.

**INDEX TERMS** Attributes learning, causal reasoning, cleaning robot, fuzzy inference network, joint learning.

## I. INTRODUCTION

With the development of society and economy, there is a huge demand for autonomous intelligent cleaning robots to replace manpower in daily life. Currently, a large number of household cleaning robots have appeared on the market and realize a certain degree of automatic operation. Although the household cleaning robots has been mass production, there are still many unsolved problems in practical application, two of which are weak intelligence and simple cleaning mode. For example, the household cleaning robot usually only has merely two operation modes, sweeping and erasing, which can only be used to clean small objects such as dust and debris. Due to the lack of perception ability of the environment and objects, the robot can only take the way of traveling the whole area, but can't selectively work on garbage area when sweeping, and this is inefficiency. Besides, it is unable

to classify and identify the garbage without visual perception ability. Therefore, the robot can't take proper cleaning mode for different garbage. In a word, the intelligent level and capability of the existing cleaning robots are far from the operation level of human beings.

In order to improve the level of intelligence of the cleaning robot, it may be useful to observe and analyze the behavior of human beings. In the process of cleaning, people usually adopt different operation modes according to the characteristics of garbage. For example, liquid is usually removed by erasing. Small and solid garbage such as paper scraps and melon shells are cleaned with sweeping mode. Grabbing mode is suitable for cleaning larger bottles and cartons. For plastic bags, the best way to clean is to perform adsorption mode. According to the above analysis, it is necessary to equip the cleaning robot with vision sensors and multiple cleaning operation modes to improve the working ability.

The aim of this paper is to realize that the cleaning robot can judge the type of garbage and take appropriate operation

The associate editor coordinating the review of this manuscript and approving it for publication was Mehul S Raval<sup>1</sup>.

mode autonomously. It is noted that the detection, identification and the analysis of attributes of garbage belong to visual perception problem. However, the decision for operation modes belong to cognition problem. Because of semantic gap between them, it is obviously difficult to directly construct a reasoning decision-making model based on garbage images. On the contrary, Human's reasoning and decision-making process is more reasonable and interpretable. When humans making decisions, they will first obtain various attributes of the object through observation, and then use rules and obtained knowledge to reason. Similarly, in order to avoid constructing an intuitive reasoning model from image to decision directly, we will realize the robot's decision-making of the garbage cleaning mode in two stages, respectively from image to attribute (visual perception), and from attribute to decision (cognitive inference). The former solves the attribute learning problem and the latter solves the problem of cognitive decision-making. Common sense tells us that the main factors influencing the decision-making of the cleaning mode are the shape, state, distribution and size of garbage. Therefore, we will firstly use the hierarchical expression ability of deep network to obtain the attributes of garbage such as state, shape, distribution, size and so on. Next, the causal relationship between the attributes and the operation modes can be built by using causal inference. Then a fuzzy inference network for operation mode decision is designed.

The main contributions of this paper are reflected in the following three aspects: (1) The proposed decision-making of the cleaning mode in this paper is very similar to human decision-making behavior, which combined perception and cognition behaviors. Thus, the proposed model has good interpretability. (2) The use of hierarchical processing greatly reduces the difficulty of the problem. It makes it possible to obtain a good autonomous decision-making of cleaning mode. (3) The introduction of causal learning technology is conducive to the joint learning of attributes and the design of fuzzy inference network.

## II. RELATED WORKS

### A. ATTRIBUTE LEARNING

Color, shape and other visual attributes play an important role in understanding and describing objects. Visual attributes are the basic characteristics of objects and the basic information obtained by people's perception of objects. People can describe objects through attribute information, but the description of objects by computers is based on data. There is a "semantic gap" between the underlying features and the high-level semantics [1]. Because visual attribute is a description of the middle-level semantics of image, it can be understood by both human and computer, Ferrari *et al.* [2] proposed the concept of "visual attributes" to solve the "semantic gap". A Farhadi *et al.* furtherly promoted visual attribute research in article "Describing Objects by their Attributes" [3]. The purpose of attribute learning is to establish the connection among underlying features,

attributes and high-level semantics. The traditional strategy of attribute learning is to train a classifier corresponding to each attribute. Early attribute learning mostly relied on hand-designed features such as SIFT, Gabor, and HOG. Considering the excellent performance of deep convolutional neural networks (DCN) in tasks such as image classification, it can play an important role in attribute extraction and learning [4], [5].

Attributes are divided into discrete nominal attributes and continuous relative attributes. For example, discrete binary attributes describe whether an object has an attribute or not. For attributes that are not easy to distinguish, they are expressed by describing the attribute strength [6]. By scoring the attribute values, the relative differences of image are determined.

There are not only correlations but also obvious differences between visual attributes. Modeling correlations and heterogeneity is an important research content for attribute learning. In early studies, these correlations between attributes have not been fully utilized, such as the indirect attribute prediction model (IAP) and direct attribute prediction model (DAP) proposed by Lampert *et al.* [7]. As an improvement, a multi-task learning-based joint attribute learning method has been developed recently. As an example, a multi task face attribute learning model for face attribute analysis is established in [8]. Because it can not only ensure the sharing of underlying features, but also meet the deliberate fine tuning of attributes, the multi-task attribute learning is usually better than single task attribute learning.

Existing attribute learning has been widely applied in the fields of face attribute analysis, image classification, visual retrieval, zero-sample learning and transfer learning. In contrast, there are few researches on intelligent decision-making. In particular, the decision-making problem of cleaning operation mode studied in this paper has not been reported publicly. When analyzing garbage attributes, this paper mainly considers four attributes: state, shape, distribution and size. Among them, the first three attributes belong to the disordered nominal feature, and the size attribute belongs to the ordered quantitative feature. For this reason, the attribute features are divided into two groups in research, and the fine-grained training is performed separately at the fully connected layer at the back end of the deep network.

### B. CAUSAL REASONING

Causality reflects the objective process of the interaction of various factors between things. In recent years, with the research results of causal inference constantly recognized by the academic community, this field is becoming a research hotspot [9]–[15]. Causal network is a common tool to infer the relationship between variables in causal reasoning. The algorithm of causal reasoning generally consists of two stages: causal skeleton learning and causal direction reasoning. Common algorithms include: score based search method, constraint based method, causal function model based method and hybrid method.

Based on the scoring search method, a causal Bayesian network structure is constructed according to certain search strategy and scoring mechanism [16]. The typical algorithm is K2 algorithm. This algorithm can search continuously until the causal network structure is obtained accurately, but for high-dimensional network, its implementation is NP hard problem.

Constraint-based algorithms can be understood as conditional independence testing methods. As early as 1990, Peter *et al.* proposed the PC (Peter-Clark) algorithm [17] and the IC (Inductive Causation) algorithm [18]. They complete the network skeleton learning of undirected graph in two stages. In 1995, Cai *et al.* [19], Pearl [20] proposed the Structural Equation Model (SEM) and Potential Outcome. Later he proposed the Structural Causal Model (SCM). The core of the framework model of potential results is to compare the results of the subjects who received the intervention with those who did not. Li [21], Schulz [22] also gives a systematic, comprehensive and in-depth introduction to the potential result model of causal reasoning. As an improvement of causal structural equation model, Shimizu [23] proposed the Linear Non-Gaussian Acyclic Model—LiNGAM (Linear Non-Gaussian Acyclic Model) and its improvement—Direct LiNGAM model [24]. Zhang *et al.* [25] proposed the SICA (ICA with Sparse Connections) method. Janzing *et al.* [26], Cai [27] proposed an Information-Geometric Causal Inference method (IGCI). It was a new method for distinguishing binary causality.

Using the Constraint-based causal reasoning algorithms, the causal framework can be constructed quickly, and then the direction of causal network can be inferred preliminarily. However, its problem is that it can't recognize Markov equivalence class. In contrast, the method based on causal function model can solve this problem. The hybrid method is just based on the combination of constraint method and causal function model. Mai *et al.* [28] proposed SADA framework. This method adopts the strategy of splitting and merging, and uses the causal network of local sparsity structure, which can accurately determine the causal variables in the case of high dimension and low sample. Szegedy *et al.* [29] proposed a causal inference algorithm CDHD for high-dimensional data. CDHD uses mutual information to find out the parent and child nodes of the target node, avoiding the huge condition set of PC algorithm, and use the mixed direction recognition algorithm to infer the direction.

### C. CLEANING ROBOTS

At present, the cleaning robots in the market are mainly floor sweeping robots, which are mainly divided into two categories: domestic floor sweeping robots and commercial floor sweeping robots used in large scenes such as airports, shopping malls, parks and urban roads. The world's first fully automatic sweeping robot is the "Trilobite" sweeping robot invented by Electrolux company. It is in the shape of a round cake, equipped with a simple sensor, can automatically avoid obstacles, and has a simple cleaning operation ability. On this

basis, many companies have developed similar sweeping robots [30], [31], which have made some improvements in the operation mechanism and operation mode, and some products have been upgraded in the degree of intelligence, equipped with vision sensor or laser radar, so that the robot has the ability of map building, path planning, positioning and navigation, and improves the operation efficiency. The cleaning robot used for large-scale scene is generally large, such as iSmart cleaning robot [32], which has four working modes of washing, sweeping, mopping and sterilization. Some robots are equipped with manipulator, which can pick up large garbage. However, due to the complexity of the open environment, large scene cleaning robots usually need manual driving. Although the domestic sweeping robot has basically realized automation, its intelligence level is relatively low, so it cannot choose the operation mode according to the types and characteristics of garbage, and the operation mode is relatively simple, usually only has the ability of sweeping or erasing, so it is difficult to deal with large-scale garbage. In order to solve these problems, this paper studies the cleaning robot with four working modes: cleaning, absorbing, grasping and erasing. The cleaning robot designed by us can take appropriate disposal mode according to the type and attribute of garbage, so as to improve its working intelligence and effect.

### D. DEEP NEURAL NETWORK

Convolutional neural network (CNN) has made great success in the field of computer vision. And the deep neural network based on convolutional neural network is present the best model to solve the problem of object detection and recognition. By end to end hierarchical feature extraction and representation learning, it can achieve the feature representation of high-level semantics. With the development of the research, many classical deep network models have been proposed. In 2012, Alexnet [33], a neural network model designed by Hinton and his student Alex krizhevsky, won the title of Imagenet competition. In 2014, GoogLeNet [34] and VGG [35] won the first and second place in the Imagenet competition. The success reason of GoogLeNet lies in the proposed Inception structure. By using serial small convolution kernel instead of large convolution kernel, the parameters of the model are effectively reduced and the convergence speed of the model is improved. Through many improvements, the Inception model has gone through four versions: V1, V2, V3 and V4. In this work, we use the Inception V3 model as the backbone of the attribute learning model.

## III. ANALYSIS OF GARBAGE ATTRIBUTES AND ITS JOINT LEARNING

### A. ANALYSIS OF GARBAGE ATTRIBUTES

Common sense shows that humans usually choose different cleaning modes according to the attributes of the garbage. Obviously, the main factors influencing the decision-making of the cleaning mode are shape, state, distribution and size.

In this paper, the state attributes mean solid or liquid; the shape attributes are non-flat or flat; the size attributes are divided into small, medium and large; the distribution attributes are overall or scattered. Correspondingly, we set four operation modes, namely sweeping, absorption, grasping and erasing mode. The sweeping mode is suitable for handling scattered, small, solid, and non-flat objects, such as melon shells, paper scraps, and glass fragments. The absorption mode is suitable for handling large flat solid objects, such as paper, plastic bags, etc. The grasping mode is suitable for handling medium- or large-size non-flat solid objects, such as cans, cartons, etc. Erasing mode is suitable for cleaning liquid objects (juice, tea, drinks) or dust.

The above-mentioned attributes are all can be obtained by visual sensors within a proper distance. Moreover, a deep network model can be used to identify these garbage attributes with the help of attribute learning technology. After the attributes are extracted, the attribute information will be input to the subsequent fuzzy decision neural network for decision-making. The flowsheet for this process is shown in Fig. 1. Among them, the dotted blue box indicates the model training process, and the red box shows the actual working process of the robot.

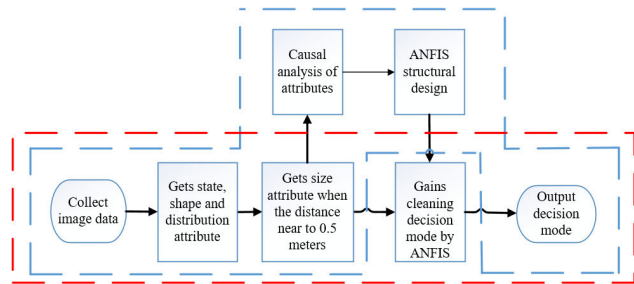


FIGURE 1. Cleaning robot working process.

It is worth noting that when the robot moves, the analysis of state, shape and distribution attributes will not have a great impact, but the size of the object will be significantly different due to the change of distance. In order to accurately evaluate the size information of the object, we agree that only when the cleaning robot is about 0.5m away from the garbage, we will extract its size attributes. Fig. 2 is a schematic diagram of the overall composition of the model.

### B. JOINT ATTRIBUTE LEARNING

Because multiple attributes are involved, and the correlation and heterogeneity between garbage attributes should be considered, therefore the study of garbage attributes in this paper will be a multi-task joint learning problem. In order to fully explore the correlation between attributes, the low-level

features of deep network model can be shared learning, while the high-level features can be fine-tuned by the strategy of divide and rule to ensure the learning of heterogeneous attributes. Among the four attributes mentioned above, the state, shape and distribution belong to the overall

appearance attributes of discrete objects, which are the disordered nominal attributes. Contrarily, the size attribute is continuous and orderly. For simplicity, the size attributes are discretized and expressed as three levels: small, medium and large. Now all attributes are discrete and orderly. In addition, the learning process of size attribute is separate from that of other attributes considering that the size attribute must be within a certain observation distance as mentioned earlier.

The network structure used to extract garbage attributes is shown in the Fig. 3, where the ImageNet image pre-trained model is used as the backbone network for attribute learning. Through the shallow part of the network, we can get the texture, edge and other low-level features. As a shared feature layer, all attributes will be adjusted during learning to ensure the relevance of the learned attributes. With the increase of network depth and the enhancement of expression ability, high-level networks gradually learn abstract high-level semantic features. In order to extract specificities related to attributes such as state, shape, distribution, and size, we remove the output layer after dense\_1 of the model and add output 1 and 2 to the full connection layer. The attributes of state, shape, and distribution are output from output 1, and the size attributes are output from output2.

Suppose that there is a training data set containing  $N$  images, where each image has  $M$  attributes. The dataset is expressed as  $X = \{X_i\}_{i=1}^N, Y = \{\{y_i^j\}_{j=1}^M\}_{i=1}^N$ . The model shown in Fig. 3 can be trained by regularizing the minimum error loss function. The joint attributes learning model DMTL based on the multi-task is shown below:

$$\arg \min_{W_c, \{W_j\}_{j=1}^M} \sum_{g=1}^2 \sum_{j=1}^{M^g} \sum_{i=1}^N \lambda^g L^g(y_i^j, F(X_i, W^g \circ W_c)) + \gamma_1 \Phi(W_c) + \gamma_2 \Phi(W^g) \quad (1)$$

where  $F(\cdot)$  is the output function of the attribute prediction after the input  $X_i$  is processed by the deep network weight calculation process.  $L^g(\cdot, \cdot)$  is the error loss function between the attribute output estimate and actual value  $y_i^j$ ;  $\Phi(\cdot, \cdot)$  is a regularization term, which is used to limit the complexity of weights.  $\gamma_k, k = 1, 2$  is the regularization representing the weight of the subnet.  $W^g, g = 1, 2$  represents the weights of the two sub-networks,  $W_c$  represents the weight of the shared network;  $M^g, g = 1, 2$  represent the attributes of the corresponding task group, where  $M^1 = \{\text{shape, state, distribution}\}, M^2 = \{\text{size}\}$ . Because the selected attributes are discrete, we choose the cross entropy loss function as follows.

$$L^g = - \sum_{j=1}^{M^g} \sum_{i=1}^N \sum_{k=1}^{C^j} (l(y_i^j, \hat{y}_i^{j,k}) \log p(\hat{y}_i^{j,k})) \quad (2)$$

where

$$p(\hat{y}_i^{j,k}) = \frac{e^{\hat{y}_i^{j,k}}}{\sum_{k=1}^{C^j} e^{\hat{y}_i^{j,k}}} \quad (3)$$

is the Softmax function.  $\hat{y}_i^{j,k}$  is the possibility that the  $j$ -th attribute value output by the attribute learning network of the

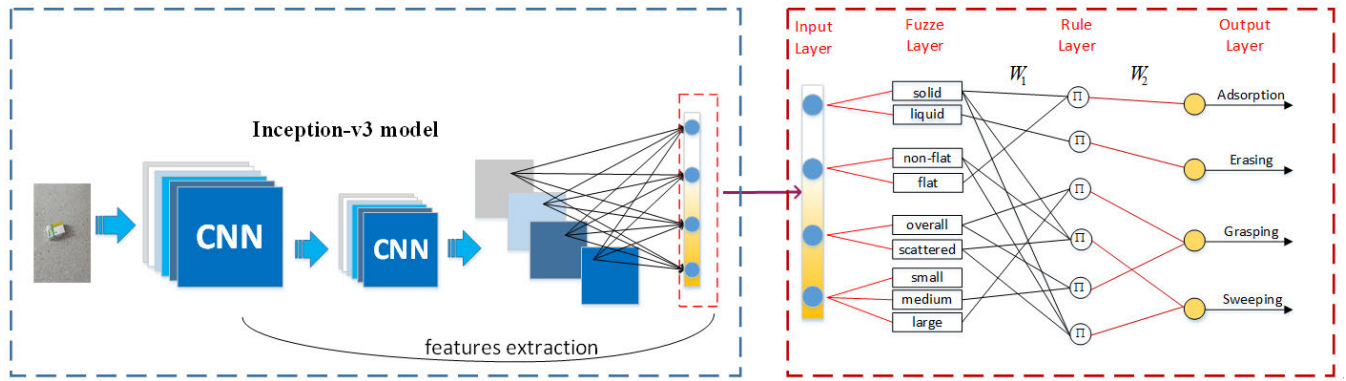


FIGURE 2. Schematic diagram of overall model composition.

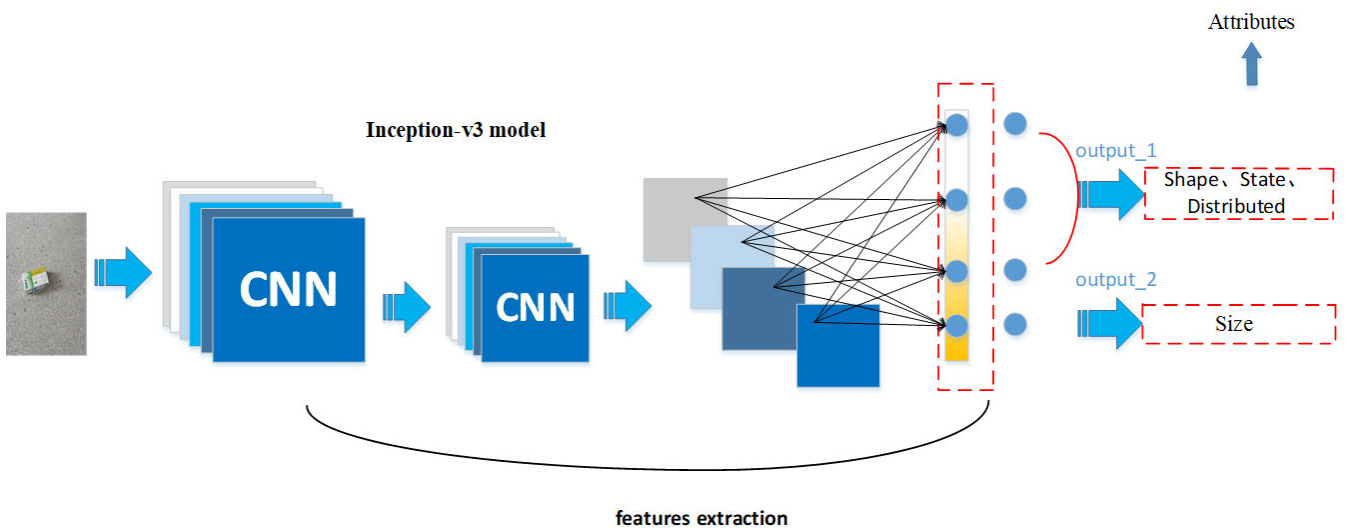


FIGURE 3. Inception-v3 based garbage attribute learning model.

$k$ -th discrete value.  $y_i^j$  is the actual value.  $l(a, b)$  is the label. When  $a = b$ , its value is 1; Otherwise, it is 0. The Inception-v3 attribute network model uses the ImageNet pre-trained model as the initialization model and gradient descent algorithm (SGD) for weight learning.

**C. CAUSAL LEARNING OF CONNECTIONS BETWEEN GARBAGE ATTRIBUTES AND OPERATION MODE DECISION**

The causal learning technology is introduced to find out which attributes affect the cleaning operation modes. These attributes will be used to guide the construction of subsequent fuzzy inference networks. In this paper, a directed acyclic graph (DAG) is used to represent the variable relationship between the cause and effect graphs, where the node connections between the cause and effect graphs are represented by directed arrows. The variable that the directed arrow points to represents the “parent node”, and the variable facing away from the directed arrow represents the “child node”. The set of nodes is denoted by  $\vec{X} = (X_1, X_2, \dots, X_P)$ . If the parent node of one node is given in DAG, then all non-child nodes

of this node are independent. According to the full probability formula and conditional independence, the joint distribution of variables of the DAG can be decomposed as follows:

$$P(X_1, \dots, X_n) = \prod_{i=1}^p P(X_i|pa_i) \tag{4}$$

where  $pa_i$  represents the set of “parent nodes” pointed to  $X_i$ . By coding the prior knowledge, we can get a local causality diagram composed of nodes and edges. If node A points to B, then A is the parent of B. We can say that the variable A is the direct cause of B. The attributes of garbage is denoted as intervention variable  $V$ , where  $V_i \in \{0, 1\}$ . The remaining attributes are denoted as  $X_i$ , where  $X_i \in \{1, 2, 3\}$ . Unobservable variables are expressed as  $U$ , and decision mode variables are denoted as  $Y_j$ , where  $Y_j \in \{0, 1\}$ . The corresponding cause-effect diagram is shown in Fig. 4. The joint distribution of DAG variables can be decomposed as follows:

$$P(X_1, X_2, X_3, U, V, Y) = P(X_1)P(X_2)P(X_3)P(U) \cdot P(V|X_1, X_2, X_3, U) \cdot P(Y|X_1, X_2, X_3, V, U) \tag{5}$$

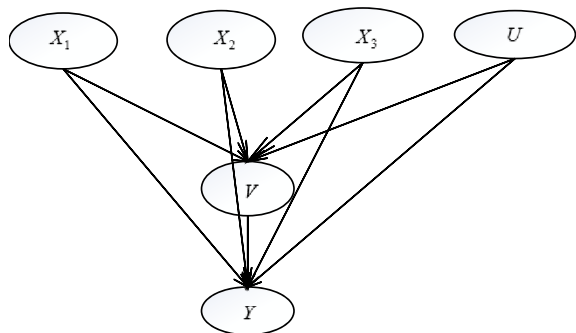


FIGURE 4. Causality diagram.

The DAG is also a data generation model, which is equivalent to the following non-parametric structure model:

$$X_i = f_i(pa_i, \alpha_i), \quad i = 1, \dots, p \quad (6)$$

In order to predict the connection between the input and output of the observation data, we need to intervene, by changing the current value of the input. The introduced “intervention operator” is expressed as  $do(X_i) = x'_i$  in DAG. Meanwhile, all the directed edges pointing to  $X_i$  in the DAG are removed and the value of  $X_i$  is set to a fixed constant when making causal estimates. As a result, a new causal expansion graph can be obtained and its joint distribution can be written as

$$P(x_1, \dots, x_n | do(X_i) = x'_i) = \frac{P(x_1, \dots, x_n)}{P(x_i | pa_i)} I(x_i = x'_i) \quad (7)$$

According to the “do” operator, the average causal effect of the binary variable  $V$  on  $Y$  is defined as

$$ACE(V \rightarrow Y) = E\{Y | do(V) = 1\} - E\{Y | do(V) = 0\} \quad (8)$$

When the causality diagram and “do” operator are known, the causal effect between the attributes of the garbage and the operation mode can be estimated. Using the “Dowhy” causal reasoning toolbox provided by Microsoft for causal analysis, the results between the garbage attributes and the operation mode decision are shown in the table below.

TABLE 1. Impact of causal learning on the operating mod.

| Attributes    | State   | Shape   | Size    | Distribution | Operation mode |
|---------------|---------|---------|---------|--------------|----------------|
| Impact factor | 0.3250  | 0.1412  | 0.2806  | 0.0093       | Adsorption     |
|               | 0.9882  | -0.0001 | -0.0052 | 0.0001       | Erasing        |
|               | -0.1062 | 0.0798  | 0.2833  | 0.3802       | Grasping       |
|               | -0.1569 | 0.0442  | 0.1141  | -0.5179      | Sweeping       |

In Table 1, the sign of impact factors indicates the direction of cause and effect. The positive value indicates the intervention is the cause, and the negative value indicates the intervention variable is the effect. The greater the absolute value is, the closer the causal relationship is. Conversely, the connection is weaker. If we ignore the case that the absolute value of the influence factor is lower than 0.1, it is easy to find out the relationships between attributes of garbage and operation modes. The attributes that affect the selection of adsorption mode are state, size and shape. For erasing mode, the decisive attribute is state. The main attributes that determines the choice of grasping include distribution, size, and state. The attributes that significantly affect the sweeping mode are state, size, and distribution. The above results have a great role in refining the decision rules, which is used to design the subsequent fuzzy inference neural network.

#### IV. FUZZY INFERENCE NETWORK FOR OPERATION MODE DECISION

In this paper, adaptive fuzzy inference neural network is used to realize the inference decision from garbage attribute to operation mode. The adaptive fuzzy inference system ANFIS [36] is a combination of a fuzzy inference system (FIS) and adaptive network. Its advantage is that it inherits the interpretability of fuzzy inference system and the learning ability of adaptive network. The network structure is shown in Fig. 5.

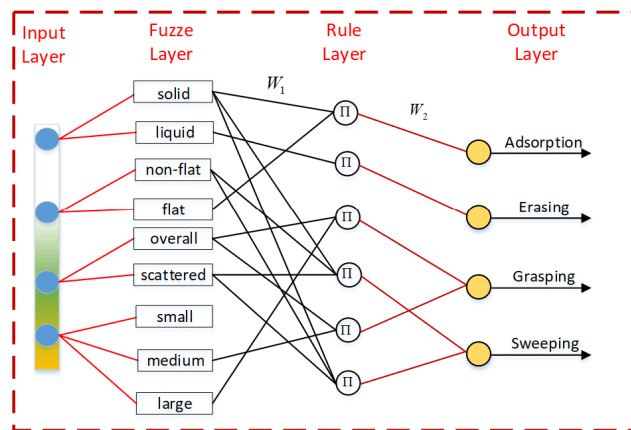


FIGURE 5. Adaptive fuzzy inference network for operation mode decision.

We redefine the rule layer, in which the number of rules is defined as six, corresponding to six rules respectively. The rules are expressed as follows:

- (1) Adsorption mode: Solid, flat objects.
- (2) Erasing mode: Liquid objects.
- (3) Grasping mode: Overall large objects.
- (4) Sweeping mode: Scattered, solid, non-flat objects.
- (5) Grasping mode: Overall and medium size objects.
- (6) Sweeping mode: Solid, whole, scattered, non-flat objects

The coding of the above rules can be expressed in matrix  $W_1$  and  $W_2$ , where  $W_1$  and  $W_2$  is a  $9 \times 6$  and  $6 \times 4$  sparse

matrix respectively. The matrix  $W_1$  represents the weight connection relationship between the fuzzy layer and the rule layer, and the matrix  $W_2$  represents the weight connection relationship between the rule layer and the decision output layer. The structure of the final ANFIS fuzzy neural network for the decision of the operation mode is shown in Fig. 5.

The network works as follows:

(1) For k-dimensional inputs  $[x_1, x_2, \dots, x_k]$ , firstly calculate the degree of membership for each input  $x_j$  variable based on the fuzzy membership function. A Gaussian membership function is used here:

$$\mu A_j^m = \exp\left[-(x_j - c_j^m)^2 / b_j^m\right] \quad (9)$$

where  $j = 1, 2, \dots, k$ ;  $m \in 1, 2, 3, c_j^m$  and  $b_j^m$  are the center and width of the membership function, respectively; k is the dimension of the input parameter. That is, the number of feature variables.

(2) Calculate the activation degree of rules by multiplication of related membership as follows:

$$w^i = a_{1,i} \mu A_1^{m_{1,i}}(x_1) * a_{2,i} \mu A_2^{m_{2,i}}(x_2) * \dots * \mu A_k^{m_{k,i}}(x_k)$$

$$i = 1, 2, \dots, r; m_{1,i} \in \{1, 2\}; m_{2,i} \in \{1, 2\};$$

$$m_{3,i} \in \{1, 2\}; m_{4,i} \in \{1, 2, 3\}; a_{k,i} \in \left\{1, \frac{1}{\mu A_k^{m_{k,i}}}\right\} \quad (10)$$

If one rule contains the  $i$ -th attribute,  $a_{k,i}$  is taken as 1. Otherwise, the inverse of the attribute membership value is taken to make the multiplication is 1.  $I_i = [a_{1,i}, \dots, a_{k,i}]^T$ ,  $W_1 = [I_1, \dots, I_r]$ .

(3) Calculate the output value of the fuzzy model based on the fuzzy calculation results:

$$y_{oc} = W_2 \cdot w^i / \sum_{i=1}^r w^i \quad (11)$$

(4) Loss calculation

$$e = \frac{1}{2} \sum_{c=1}^4 (y_{dc} - y_{oc})^2 \quad (12)$$

where the  $y_{dc}$  is the expected output of the network and the  $y_{oc}$  is actual network output.

### V. EXPERIMENTAL RESULTS AND ANALYSIS

#### A. EXPERIMENTAL DATA SET AND ENVIORNMENT

There are many kinds of garbage in home environment, with big differences in color, shape and size. How to choose the attribute reasonably is the precondition of robot intelligent cleaning. For simplicity, only four attributes of state, shape, size and distribution are considered in this paper. In the experiment, we chose 25 kinds of garbage which are common in our life as the experimental objects. Since there is no related public data set, the data used in the experiment is collected by ourselves in the actual home environment. There are 1513 images in the dataset, and each image usually contains only one kind of garbage. Among them, there are 911 pictures taken at a fixed distance of 0.5 meters and 602 pictures taken at a non-fixed distance. In order to increase the sample size

of network training, the image data enhancement tool Image Data Generator provided by Keras is used in the experiment to perform horizontal mirror flip, random rotation, cropping, scaling and other processing on the training samples. Finally, the total number of sample images is expanded to 6052, of which 3644 pictures are generated with fixed distance. When training networks models, 60% of the total samples are used as training samples, 20% of the total samples are used as test samples, and the remainder samples are used as validation samples. It is noted that the total samples selected for size attribute network model training and testing come from 3644 pictures generated with fixed distance. The Label-img tool is used to mark the attributes of the all enhanced garbage images and the operation decision modes. Some examples of garbage samples are shown in Fig. 6, and Table 2 is corresponding garbage attribute information.

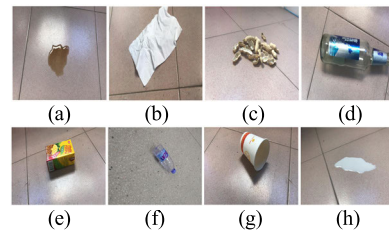


FIGURE 6. Examples of garbage samples.

TABLE 2. Corresponding attributes of garbage samples.

| State |        | Shape    |      | Size  |        |       | Distribution |           | Operation mode |
|-------|--------|----------|------|-------|--------|-------|--------------|-----------|----------------|
| solid | liquid | non-flat | flat | small | medium | large | overall      | scattered |                |
|       | √      |          | √    |       | √      |       | √            |           | Adsorption     |
| √     |        |          | √    |       | √      |       | √            |           | Adsorption     |
| √     |        | √        |      | √     |        |       |              | √         | Sweeping       |
| √     |        | √        |      |       |        |       | √            | √         | Grasping       |
| √     |        | √        |      |       | √      |       | √            |           | Grasping       |
| √     |        | √        |      |       | √      |       | √            |           | Grasping       |
| √     |        | √        |      |       | √      |       | √            |           | Grasping       |
|       | √      |          | √    |       | √      |       | √            |           | Erasing        |

The hardware platform for attribute learning model training includes Intel Core i7-7700k CPU, two GeForce GTX1080Ti GPUs, one 16G Kingston memory. In the software environment, we use Ubuntu 16.04 as the system, which is equipped with Keras and Tensorflow1.8 deep learning framework.

#### B. ATTRIBUTE LEARNING

We compared different attribute learning schemes, including attribute learning in single task mode, multi-task attribute learning without grouping, and grouped multi-task attribute learning considering heterogeneity.

Single task mode attribute learning, that is, each attribute is learned by a special model. The complete model is composed

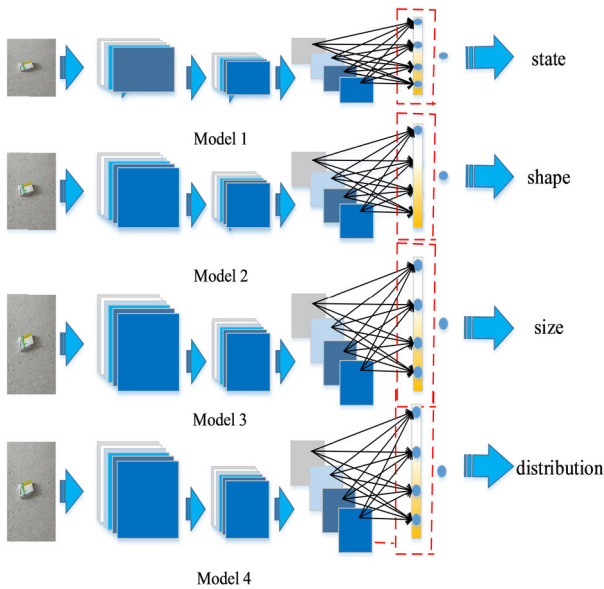


FIGURE 7. Single task learning model.

TABLE 3. Confusion matrix for Single task mode attribute learning.

| Attributes | solid | liquid | non-flat | flat | overall | scattered | small | medium | large |
|------------|-------|--------|----------|------|---------|-----------|-------|--------|-------|
| solid      | 293   | 3      |          |      |         |           |       |        |       |
| liquid     | 9     | 1633   |          |      |         |           |       |        |       |
| non-flat   |       |        | 582      | 2    |         |           |       |        |       |
| flat       |       |        | 299      | 1055 |         |           |       |        |       |
| overall    |       |        |          |      | 4       | 355       |       |        |       |
| scattered  |       |        |          |      | 443     | 1136      |       |        |       |
| small      |       |        |          |      |         |           | 332   | 4      | 0     |
| medium     |       |        |          |      |         |           | 7     | 295    | 2     |
| large      |       |        |          |      |         |           | 0     | 0      | 88    |

of 4 Inception networks, as shown in Fig. 7. the confusion matrix of each attribute on the test set under this scheme is shown in Table 3 & Table 6.

From the results, it can be seen that the accuracy of state attributes test is 99.38%, and the accuracy of the shape attribute test is only 84.47%. Among them, flat objects are more likely to be misjudged, and about 22% are misjudged as non-flat objects. In contrast, the accuracy of the distribution attribute test is only 58.82%. Almost all the overall object is misjudged as a scattered object. The error rate in discrimination reaches 98.9%. In addition, 28% of the scattered objects are misjudged. For the size attributes testing, the accuracy rate reached 98.21%. The results show that the single-task attribute learning model is effective for learning state, distribution, and size attributes. However, it is not suitable for distribution attribute training, and it is difficult to accurately distinguish the overall and the scattered objects. Fig. 3. shows the multi-task attribute learning model without grouping.

An inception network is used to train multiple attributes at the same time in the way of multi-task joint learning. Firstly, all samples are used to train the state, shape, and distribution attributes. During the training process, we will first train the weight parameters of the size attribute subnetwork, and the initial learning rate is set to 0.005. After that, the samples taken at a fixed distance are used to train the size attributes. Meanwhile, the obtained previously weight parameters of the network connection are fixed, and the initial learning rate is set to 0.0025. The resulting property test confusion matrix is shown in Table 4 & Table 6. It can be seen that, although the accuracy rate of size attribute test is decreased compared with single task learning, its accuracy rate on the shape and distribution attributes has been greatly improved.

TABLE 4. Confusion matrix for ungrouped multi-task attribute.

| Attributes | solid | liquid | non-flat | flat | overall | scattered | small | medium | large |
|------------|-------|--------|----------|------|---------|-----------|-------|--------|-------|
| solid      | 292   | 4      |          |      |         |           |       |        |       |
| liquid     | 5     | 1637   |          |      |         |           |       |        |       |
| non-flat   |       |        | 562      | 22   |         |           |       |        |       |
| flat       |       |        | 21       | 1333 |         |           |       |        |       |
| overall    |       |        |          |      | 349     | 10        |       |        |       |
| scattered  |       |        |          |      | 11      | 1568      |       |        |       |
| small      |       |        |          |      |         |           | 319   | 17     | 0     |
| medium     |       |        |          |      |         |           | 11    | 286    | 7     |
| large      |       |        |          |      |         |           | 0     | 2      | 86    |

Finally, all attributes are divided into two groups for joint learning separately. Considering that the size attribute is ordered, it is regarded as a group alone. The confusion matrix obtained from the grouped multiple tasks joint learning model of attributes is shown in Table 5 & Table 6. The results show that the Compared with first two attribute learning schemes, the accuracy of the grouped multi-task joint learning has significantly improved because it considers both the correlation of the attributes and the heterogeneity of the attributes. accuracy of tests respectively reaches 99.74%, 97.78%, 98.90% and 99.38% for state, shape, size and distribution attribute. For the comparison, the final statistical test results of attribute learning methods are listed in Table 6.

C. METHOD COMPARISON

In this section, the proposed method in this paper is compared with other methods. The first method to be compared is the direct method which directly uses the Inception-V3 deep network for operation mode decision without attribute learning (Fig. 8). It directly completes the mapping from the image to the decision space through learning. The result shows that the test accuracy of this method is 92.32%.

In addition, considering that decision trees, SVMs, and fuzzy neural networks are common inference methods, the performance of these methods combined with attribute learning is tested and compared. Finally, the improved fuzzy inference network method combined with causal inference and



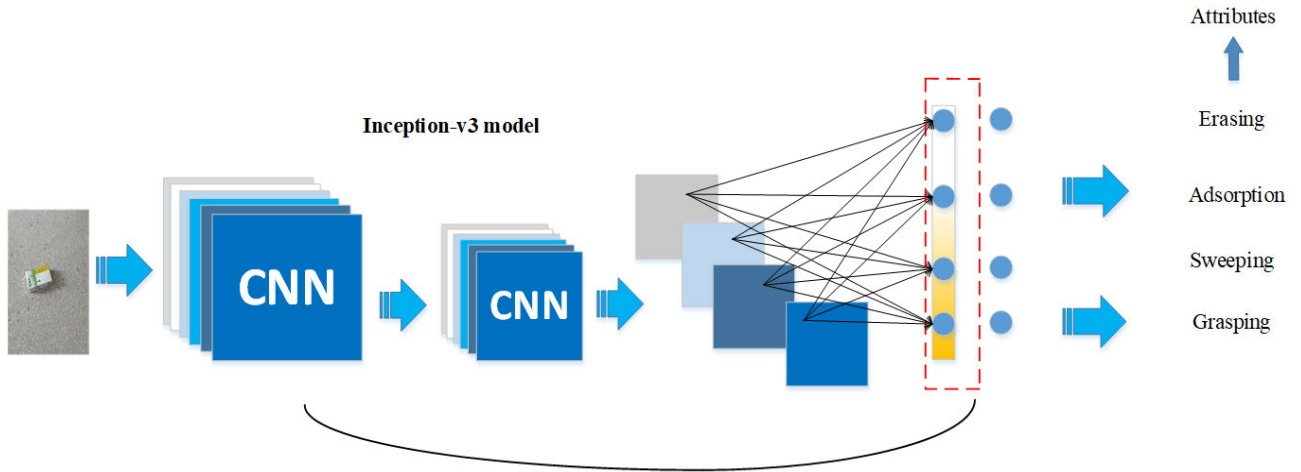


FIGURE 8. Direct modeling of the operation mode decision based on the Inception-V3 neural network.

TABLE 5. Confusion matrix for grouped multi-task joint attribute learning.

| Attributes | solid | liquid | non-flat | flat | overall | scattered | small | medium | large |
|------------|-------|--------|----------|------|---------|-----------|-------|--------|-------|
| solid      | 296   | 0      |          |      |         |           |       |        |       |
| liquid     | 5     | 1637   |          |      |         |           |       |        |       |
| non-flat   |       |        | 560      | 24   |         |           |       |        |       |
| flat       |       |        | 19       | 1335 |         |           |       |        |       |
| overall    |       |        |          |      | 354     | 5         |       |        |       |
| scattered  |       |        |          |      | 7       | 1572      |       |        |       |
| small      |       |        |          |      |         |           | 331   | 5      | 0     |
| medium     |       |        |          |      |         |           | 2     | 302    | 0     |
| large      |       |        |          |      |         |           | 0     | 1      | 87    |

TABLE 6. Attribute detection accuracy with different attribute learning models (%).

| Attributes   |           | Single task model | Ungrouped multi-task model | Grouped multi-task joint model |
|--------------|-----------|-------------------|----------------------------|--------------------------------|
| state        | solid     | 98.99             | 98.65                      | 100                            |
|              | liquid    | 99.45             | 99.70                      | 99.70                          |
| shape        | non-flat  | 99.66             | 96.23                      | 95.89                          |
|              | flat      | 77.92             | 98.45                      | 98.60                          |
| distribution | overall   | 0.01              | 97.21                      | 98.61                          |
|              | scattered | 71.94             | 99.30                      | 99.56                          |
|              | small     | 98.81             | 94.94                      | 98.51                          |
| size         | medium    | 97.04             | 94.08                      | 99.34                          |
|              | large     | 100               | 97.73                      | 98.86                          |

attribute learning proposed in this paper is tested. The final test results of various methods are listed in Table 7. The results show that the decision accuracy of the decision tree

TABLE 7. Results of the accuracy of various methods.

| methods  | Accuracy (%) |
|--|--------------|
| Direct mode decision based on deep learning                    | 92.32        |
| Attribute Learning + Decision Tree                             | 97.23        |
| Attribute Learning + Fuzzy Neural Network                      | 98.01        |
| Attribute Learning + SVM                                       | 97.68        |
| Attribute learning + causal reasoning + improved ANFIS network | 98.01        |

TABLE 8. ANFIS test results with different rule layers (%).

| Epoch(1000) | 2     | 3     | 4     | 5     | 6     | 7     | 8     | 9     | 10    | 11    | 12    | 13    | 14    | 15    | Loss | Time(s) |
|-------------|-------|-------|-------|-------|-------|-------|-------|-------|-------|-------|-------|-------|-------|-------|------|---------|
| Rules       | 7.59  | 22.60 | 45.87 | 63.53 | 74.42 | 97.52 | 97.52 | 97.52 | 94.38 | 94.38 | 94.38 | 94.38 | 94.38 | 94.38 | 0.05 | 92      |
| 4           | 29.20 | 26.07 | 26.07 | 46.36 | 48.67 | 48.34 | 74.58 | 74.58 | 74.58 | 74.58 | 87.62 | 87.62 | 97.02 | 97.02 | 0.18 | 88      |
| 6           | 61.38 | 64.52 | 94.88 | 94.88 | 94.88 | 94.88 | 94.88 | 94.88 | 94.88 | 94.88 | 94.88 | 94.88 | 94.88 | 94.88 | 0.03 | 80      |
| 8           | 91.08 | 93.39 | 93.89 | 93.89 | 97.02 | 97.02 | 98.01 | 98.01 | 98.01 | 98.01 | 98.01 | 98.01 | 98.01 | 98.01 | 0.02 | 96      |
| 10          | 48.34 | 63.69 | 93.06 | 98.01 | 83.49 | 98.01 | 98.01 | 98.01 | 98.01 | 98.01 | 98.01 | 98.01 | 98.01 | 98.01 | 0.04 | 92      |
| 12          | 94.88 | 94.88 | 98.01 | 98.01 | 98.01 | 98.01 | 98.01 | 98.01 | 98.01 | 98.01 | 98.01 | 98.01 | 98.01 | 98.01 | 0.01 | 50      |
| 14          | 95.70 | 98.01 | 98.01 | 98.01 | 98.01 | 98.01 | 98.01 | 98.01 | 98.01 | 98.01 | 98.01 | 98.01 | 98.01 | 98.01 | 0.04 | 99      |
| 16          | 41.58 | 62.54 | 88.61 | 93.23 | 98.01 | 98.01 | 98.01 | 98.01 | 98.01 | 98.01 | 98.01 | 98.01 | 98.01 | 98.01 | 0.02 | 119     |
| 18          | 48.34 | 62.87 | 64.68 | 79.86 | 93.89 | 94.88 | 98.01 | 98.01 | 98.01 | 98.01 | 98.01 | 98.01 | 98.01 | 98.01 | 0.02 | 103     |
| 20          | 79.37 | 79.37 | 79.37 | 79.37 | 79.37 | 98.01 | 98.01 | 98.01 | 98.01 | 98.01 | 98.01 | 98.01 | 98.01 | 98.01 | 0.01 | 144     |
| 22          | 2.31  | 43.56 | 61.22 | 61.22 | 61.22 | 61.22 | 61.22 | 90.42 | 92.73 | 97.52 | 97.52 | 97.52 | 97.52 | 97.52 | 0.02 | 152     |
| 24          | 16.83 | 61.22 | 61.22 | 85.80 | 86.79 | 86.79 | 86.79 | 86.79 | 86.79 | 86.79 | 86.30 | 86.30 | 84.98 | 49.87 | 0.03 | 160     |

is 97.23% and the accuracy of the SVM decision is 97.68%. Note that the performance of fuzzy neural networks is related to the number of hidden rule layer neurons. Thus we test the results of fuzzy neural networks with different number of rules (Table 8).

It can be found that when the number of rules is 8-20, the network can get the best result 98.01% in 10000 iterations.

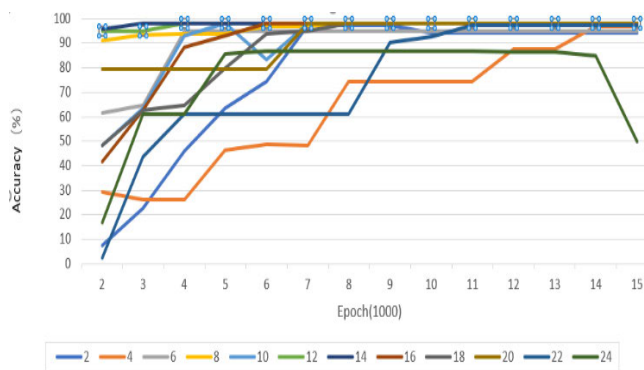


FIGURE 9. ANFIS test results with different rule layers(%).

In particular, when the number of rules is 10-14, the network performance is optimal. Considering stability, accuracy and convergence rate, the number of rules of adaptive fuzzy neural network is set to 12 in the experiment, and the total number of network parameters to be learned is 96. It is noted that there is still redundancy in the number of rules. In contrast, there are only six rules in the rule layer of ANFIS fuzzy reasoning network based on the causal analysis proposed in this paper, and only 37 parameters need to be trained. Moreover, the system is stable after 6000 iterations, and the accuracy can reach the best value 98.01% at present. The ANFIS test results with different rule layers are shown in Fig.9.

## VI. CONCLUSION

According to the characteristics of garbage, this paper proposes a cleaning robot operation mode decision model based on attribute learning and related attribute causal reasoning. The decision-making process is divided into two stages. In the first stage, the powerful feature representation ability of neural network is used to imitate the way of human analysis and dispose garbage according to the "attribute" feature. In the second stage, the reasoning network simplifies the structure design with the help of causal analysis. The parameters to be learned in the model are reduced by nearly two-thirds compared with the conventional fuzzy neural network, and it has good interpretability. The above scheme effectively avoids the semantic gap in the direct reasoning scheme. Finally, the cleaning mode decision-making model is deployed on the mobile robot and tested in the laboratory environment. In most cases, the cleaning robot can give the decision-making mode consistent with the human, which basically meets the expected requirements.

Although the proposed method has achieved good results, there is still room for improvement. At present, we only quantify the size attributes in our method, but in fact, it is more appropriate to describe the size attributes with continuous values. In order to get better training effect, it is considered to relabel the size attributes and set a separate loss function. In addition, the connection between attributes and cleaning operation modes can also be used to guide the design

of attribute learning network. These issues will be further improved in our future work.

Considering the complexity of the home environment and the fact that the designed cleaning robot can only work on the plane ground at present, we mainly focus on the cleaning of the common garbage on the ground. The garbage on the tables or steps is not considered at present. Moreover, in order to simplify the problem, such garbage mixed stacking situation is not considered in this paper for the time being. This situation obviously cannot be handled by a single operation mode. It can only be handled by combining multiple operation modes. These are our future research works.

## REFERENCES

- [1] P.-Y. Yin, B. Bhanu, K.-C. Chang, and A. Dong, "Integrating relevance feedback techniques for image retrieval using reinforcement learning," *IEEE Trans. Pattern Anal. Mach. Intell.*, vol. 27, no. 10, pp. 1536–1551, Oct. 2005.
- [2] V. Ferrari and A. Zisserman, "Learning visual attributes," in *Proc. Adv. Neural Inf. Process. Syst.*, 2007, pp. 440–443.
- [3] A. Farhadi, I. Endres, D. Hoiem, and D. Forsyth, "Describing objects by their attributes," in *Proc. IEEE Conf. Comput. Vis. Pattern Recognit.*, Jun. 2009, pp. 1778–1785.
- [4] A. S. Razavian, H. Azizpour, J. Sullivan, and S. Carlsson, "CNN features off-the-shelf: An astounding baseline for recognition," in *Proc. IEEE Conf. Comput. Vis. Pattern Recognit. Workshops*, Jun. 2014, pp. 512–519.
- [5] J. Donahue, Y. Jia, O. Vinyals, J. Hoffman, N. Zhang, E. Tzeng, and T. Darrell, "DeCAF: A deep convolutional activation feature for generic visual recognition," in *Proc. Int. Conf. Mach. Learn. (ICML)*, 2014, pp. 647–655.
- [6] D. Parikh and K. Grauman, "Relative attributes," in *Proc. Int. Conf. Comput. Vis.*, Nov. 2011, pp. 503–510.
- [7] C. H. Lampert, H. Nickisch, and S. Harmeling, "Learning to detect unseen object classes by between-class attribute transfer," in *Proc. IEEE Conf. Comput. Vis. Pattern Recognit.*, Jun. 2009, pp. 951–958.
- [8] H. Han, A. K. Jain, F. Wang, S. Shan, and X. Chen, "Heterogeneous face attribute estimation: A deep multi-task learning approach," *IEEE Trans. Pattern Anal. Mach. Intell.*, vol. 40, no. 11, pp. 2597–2609, Nov. 2018.
- [9] O. James, S. R. Jilke, and G. G. Van Ryzin, *Experiments in Public Management Research: Challenges and Contributions* (Prospects for Experimental Approaches to Research on Bureaucratic Red Tape). 2017, pp. 219–243.
- [10] J. Pearl et al., "Causal inference in statistics," *J. Exp. Psychol.*, vol. 136, pp. 23–42, 2007.
- [11] G. W. Imbens and D. B. Rubin, *Causal Inference for Statistics, Social, and Biomedical Sciences: An Introduction*. Cambridge, U.K.: Cambridge Univ. Press, 2015, pp. 461–476.
- [12] J. Pearl, *Causality: Models, Reasoning, and Inference*. Cambridge, U.K.: Cambridge Univ. Press, 2000.
- [13] S. L. Morgan and C. Winship, *Counterfactuals and Causal Inference: Methods and Principles for Social Research*. Cambridge, U.K.: Cambridge Univ. Press, 2014, pp. 188–225.
- [14] J. D. Angrist and J.-S. Pischke, "Undergraduate econometrics instruction: Through our classes, darkly," *J. Econ. Perspect.*, vol. 31, no. 2, pp. 125–144, May 2017.
- [15] P. W. Battaglia et al., "Relational inductive biases, deep learning, and graph networks," 2018, *arXiv:1806.01261*. [Online]. Available: <http://arxiv.org/abs/1806.01261>
- [16] G. F. Cooper and E. Herskovits, "A Bayesian method for the induction of probabilistic networks from data," *Mach. Learn.*, vol. 9, no. 4, pp. 309–347, Oct. 1992.
- [17] S. Peter, G. Clark, and S. Richard, *Causation, Prediction, and Search*. Cambridge, MA, USA: MIT Press, 1996.
- [18] T. Verma and J. Pearl, "Equivalence and synthesis of causal models," in *Proc. 6th Conf. Uncertainty Artif. Intell.*, 1990, pp. 255–268.
- [19] R. C. Cai, W. Chen, K. Zhang, and Z. F. Hao, "Summary of causal discovery based on non-sequential observation data," *Chin. J. Comput.*, vol. 40, no. 6, pp. 1470–1490, 2017.

- [20] J. Pearl, "Probabilistic reasoning in intelligent systems: Networks of plausible inference," *Comput. Sci. Artif. Intell.*, vol. 70, no. 2, pp. 1022–1027, 1996.
- [21] W. Z. Li, "Potential result model in causal reasoning: Origin, logic and implication," *Public Admin. Rev.*, pp. 124–149, 2018.
- [22] M. Schulz, *Counterfactuals and Probability*. New York, NY, USA: Oxford Univ. Press, 2017.
- [23] S. Shimizu, "Lingam: Non-Gaussian methods for estimating causal structures," *Behaviormetrika*, vol. 41, no. 1, pp. 54–98, 2014.
- [24] S. Shimizu, T. Inazumi, Y. Sogawa, A. Hyvärinen, Y. Kawahara, T. Washio, P. O. Hoyer, and K. Bollen, "A direct method for learning a linear non-Gaussian structural equation mode," *J. Mach. Learn. Res.*, vol. 12, no. 2, pp. 1225–1248, 2011.
- [25] K. Zhang, H. Peng, L. Chan, and A. Hyvarinen, "ICA with sparse connections: Revisited," in *Independent Component Analysis and Signal Separation*. 2009, pp. 195–202.
- [26] D. Janzing, J. Mooij, K. Zhang, J. Lemeire, J. Zscheischler, P. Daniušis, B. Studel, and B. Schölkopf, "Information-geometric approach to inferring causal directions," *Artif. Intell.*, vols. 182–183, no. 5, pp. 1–21, 2012.
- [27] R. Cai, Z. Zhang, and Z. Hao, "Sada: A general framework to support robust causation discovery," in *Proc. ICML*, 2013, pp. 208–216.
- [28] G. Mai, S. Peng, Y. Hong, and P. Chen, "Fast causal division for supporting high dimensional causal discovery," in *Proc. IEEE Int. Conf. Comput. Sci. Eng. (CSE) IEEE Int. Conf. Embedded Ubiquitous Comput. (EUC)*, Jul. 2017, pp. 291–296.
- [29] C. Szegedy, V. Vanhoucke, S. Ioffe, J. Shlens, and Z. Wojna, "Rethinking the inception architecture for computer vision," in *Proc. IEEE Conf. Comput. Vis. Pattern Recognit. (CVPR)*, Jun. 2016, pp. 2818–2826.
- [30] B. Gao, "Research on key technologies of indoor Intelligent sweeping robot," Chongqing Univ., Chongqing, China, Tech. Rep., 2017.
- [31] X. X. Sun and Y. S. Zhao, "Research on the development status and trend of sweeper robots," *Sci. And Technol. Inf.*, no. 28, pp. 238–239, 2017.
- [32] K. Ning, Z. DongBo, F. Yin, and H. H. Xiao, "Garbage detection and classification of intelligent sweeping robot based on visual perception," *Chin. J. Image Graph.*, vol. 24, no. 8, pp. 1358–1368, 2019.
- [33] C. Szegedy, W. Liu, Y. Jia, P. Sermanet, S. Reed, D. Anguelov, D. Erhan, V. Vanhoucke, and A. Rabinovich, "Going deeper with convolutions," in *Proc. IEEE Conf. Comput. Vis. Pattern Recognit. (CVPR)*, Jun. 2015, pp. 1–9.
- [34] P. De Boer, D. P. Kroese, S. Mannor, and R. Y. Rubinstein, "A tutorial on the cross-entropy method," *Ann. Oper. Res.*, vol. 134, no. 1, pp. 19–67, 2005.
- [35] A. Krizhevsky, I. Sutskever, and G. E. Hinton, "ImageNet classification with deep convolutional neural networks," in *Proc. Adv. Neural Inf. Process. Syst. (NIPS)*, vol. 2012, pp. 1097–1105.
- [36] C.-T. Sun, "Rule-base structure identification in an adaptive-network-based fuzzy inference system," *IEEE Trans. Fuzzy Syst.*, vol. 2, no. 1, pp. 64–73, 2nd Quart., 1994.



**YAPENG LI** is currently pursuing the master's degree in control science and control engineering with Xiangtan University. His research interests include image processing, pattern recognition, robot behavior decision-making, and deep learning.



**DONGBO ZHANG** received the M.S. degree in computer application technology and the Ph.D. degree in control science and engineering from Hunan University, China. He has been a Professor with the College of Information Engineering, Xiangtan University, since 2006. His research interests include pattern recognition, image processing, machine learning, and machine intelligence.



**FENG YIN** received the B.S. degree from Xiangtan University, China, in 2004, and the M.S. degree and the Ph.D. degree in control science and technology from Hunan University, China, in 2008 and 2013, respectively. In 2013, he was with Xiangtan University, as a Lecturer. His current research interests include pattern recognition, computing vision, machine learning, and mobile robot.



**YING ZHANG** received the M.S. degree in control theory and control engineering from the School of Automation, Guangdong University of Technology, China, and the Ph.D. degree in control science and engineering from the School of Electrical and Information Engineering, Hunan University. His research interests include robot control, pattern recognition, and intelligent control.

...